Optimization of CO2 Finned Tube Gas Coolers: Advancements in Design and Performance

[1]Mandvi Rajak, [2]Mr. Deepak Solanki

[1]Department of Mechanical Engineering, Astral Institute of Technology & Research, Indore, (M.P.)

[2]Department of Mechanical Engineering, Astral Institute of Technology & Research, Indore, (M.P.)

Email mandvirajak.98@gmail.com

* Corresponding Author: Mandvi Rajak

Abstract: *This research paper explores the evolving use of CO2 as an eco-friendly refrigerant in cooling and heat pump systems, focusing on the design and efficiency of CO2-based trans-critical cooling cycles with fin-and-tube gas coolers. The paper highlights the challenges in high-temperature environments, emphasizing the need for efficient gas cooler designs in warm and humid conditions, like those in India. Various types of plate fin heat exchanger surfaces are examined, including plain, perforated, louvered, wavy, offset strip, and pin fins. The paper presents a comprehensive study combining mathematical and computational fluid dynamics (CFD) analyses to enhance the heat transfer performance of CO2 finned tube gas coolers. It aims to predict CO2 refrigerant temperature profiles and improve the overall design for better heat transfer efficiency.*

Keywords: *CO2 Refrigeration, Trans-critical Cooling Cycles, Fin-and-Tube Gas Coolers, Heat Exchanger Surfaces, Computational Fluid Dynamics, Thermal Efficiency, Eco-Friendly Cooling Agents.*

I. INTRODUCTION

CO2 has re-emerged as an eco-friendly and nature-derived cooling agent choice for cooling and heat pump systems, appreciated for its excellent thermal properties and low Global Warming Potential (GWP). These systems function in either subcritical or trans-critical cycles, with the choice contingent on the surrounding temperature conditions. Nonetheless, high-temperature environments present specific challenges to this operation. In warm and humid environments like those in India, systems need to function within the trans-critical cycle because CO2's comparatively low critical temperature. As a result, heat is expelled inside the supercritical area avoiding condensation in the gas cooler. In warmer conditions, the layout, and operation of the gas cooler are particularly vital, greatly affecting the system's overall efficiency. The gas cooler is acknowledged as a crucial element that markedly affects the performance of these systems [1]. In CO2-based trans-critical cooling cycles fin-and-tube gas coolers are prevalently used due to their straightforward design, robustness, and cost efficiency. The efficacy of such heat exchangers is crucial within their systems and there's an ongoing need for enhancement. Over recent decades, extensive research, both experimental and theoretical, has been conducted on finned-tube gas coolers. This research aims to deepen understanding of fluid heat transfer and friction dynamics, thereby improving their performance. Techniques like the distributed method for mapping CO2 temperature profiles along the flow direction in a finned-tube gas cooler and the tubby-tube approach for simulating the performance of finned-tube air-to-refrigerant evaporators, including the calculation of refrigerant thermodynamic properties, have been developed. These approaches are also applicable in the modeling of CO2 gas coolers. The geometric parameters of these coolers, which significantly affect their performance, have been thoroughly examined and optimized using Computational Fluid Dynamics (CFD) modeling. However, it's important to note that most of these studies are based on uniform airflow conditions, which may differ from real-world scenarios. [2].

Table 1 Specification of the Modelled Gas Cooler

DIMENSIONS	
W x H x D	0.61 x 0.46 x 0.05
Front Area(M^2)	0.281
Fin Shape	Raised lance
Fin Pitch(mm)	1.5
Fin Thickness(mm)	0.13
Number Of Tubes Row	3
Tube outside Diameter(mm)	7.9
Tube Inside Diameter(mm)	7.5
Tube Shape	smooth

1.1 Varieties of Plate Fin Heat Exchanger Surfaces

Heat exchangers with plate fins commonly utilize extended surfaces to compensate for the lower heat transfer coefficient on the gas side. These extended surfaces are designed to enhance heat transfer coefficients. To achieve this, fins with specialized geometries have been created, providing significantly higher heat transfer coefficients compared to extended plain surfaces. However, these specialized designs can sometimes lead to increased pressure drops. Various types of several extended surfaces have been created, such as louvered, wavy offset, plain rectangular, and plain trapezoidal surfaces, among others. In our numerical and ex perimental work, we focus on the offset strip fin geometry.

A. Plain Fins: These are flat, untextured surfaces, commonly used for fluids with little to no fouling. They offer a straightforward design and are easy to manufacture.

B. Perforated Fins: A pattern of evenly spaced holes is punched into the fin material to create the perforated fins. The fin material is then folded to create the flow channels. Featuring small holes, these fins promote increased turbulence in the fluid flow, which enhances heat transfer. They are particularly effective for fluids with moderate viscosity.

C. Louvered Fins: These fins have small cuts that create a louvered pattern. The design increases surface area and turbulence, improving the heat transfer rates. They're well-suited for air-to-liquid heat exchange. High Reynolds number values cause the fluid to flow along the direction of the louvers, resulting in boundary layer flow, whereas low Reynolds numbers cause the stream to flow parallel to the axial direction (duct flow).

D. Wavy Fins: Wavy fins are shaped like plain fins in cross-section, but they are curved in the direction that the fluid flows. Upon crossing the concave, wavy surface, the fluid, the resulting wave-like structures in the wavy fins create a complicated flow field and effective interruptions that eventually culminate in the formation of a vortex. With a corrugated shape, these fins create a more turbulent flow, enhancing heat transfer. The wavy design is beneficial for applications with high heat transfer requirements.

E. Offset Strip Fins: Comprising of lanced strips offset from each other, these fins disrupt the flow, significantly increasing the heat transfer coefficient. This design is effective in compact heat exchangers.

F. Pin Fins: These consist of small pins that extend from the plate surface, expanding the area covered and the heat transfer. They are ideal for high-temperature and high-pressure applications.

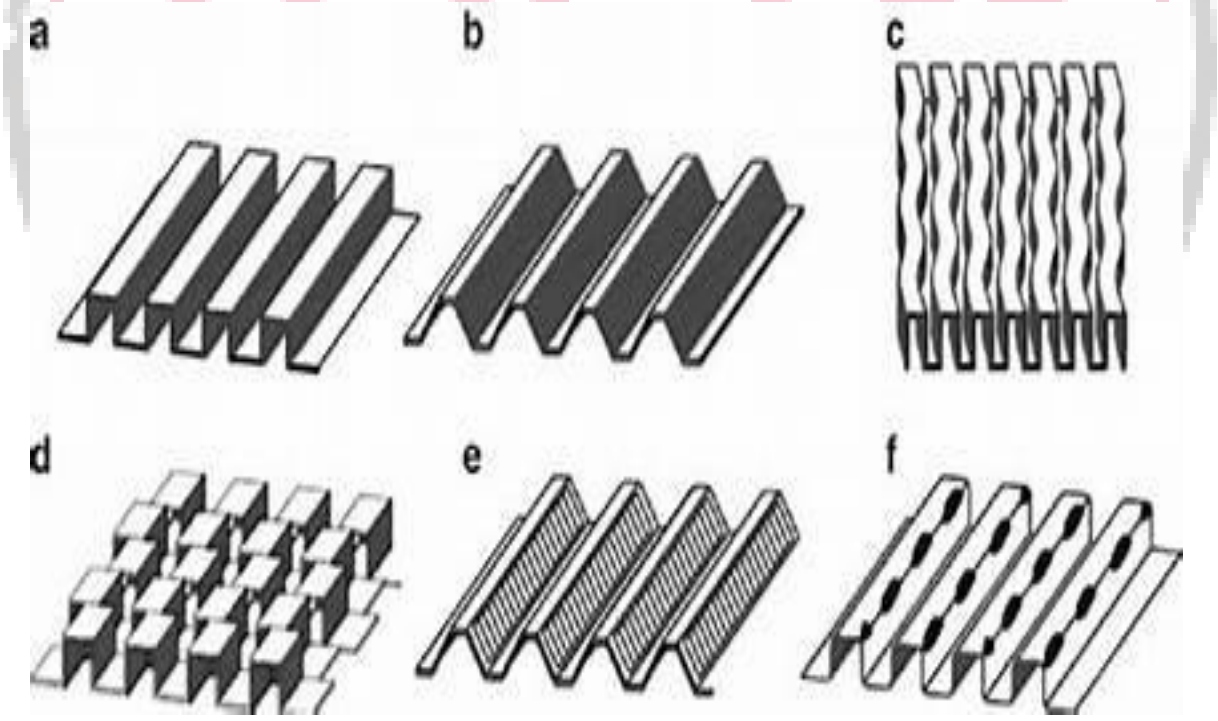

Figure 1 Distinctive Plate Fin Heat Exchanger Surface Types

Most people associate carbon dioxide (CO2) with the respiration or combustion of fossil fuels, and the atmosphere's high concentration of CO2 is one of the main causes of global warming. Natural sinks like forests primarily regulate the amount of CO2 in the atmosphere, but the growing trend of deforestation is raising the amount of CO2 in the atmosphere even more. Utilizing carbon capture methods to move CO2 to storage areas, like subterranean geological reservoirs, is another way to manage the concentration of CO2. These reservoirs, however, have a finite amount of capacity. In this sense, it might be utilized as a substitute for other widely used fluids to lessen the quantity of CO2 that needs to be kept. CO2, for example, can be used [3]. Because the gas cooler has a large energy loss, it impacts the CO2 refrigeration systems in a major way. Since such, it is deemed essential to conduct additional research and design it appropriately [4].

1.2 Advancements in CO2 Cycle Technology

The swift advancement of modern society has led to substantial production of carbon dioxide (CO2) in various industrial processes. These include Natural gas, coal, and coke combustion, the production of cement and lime, as well as the fermentation of sugars and carbohydrates, among others. Annually, over There is an atmospheric emission of 30 billion tons of CO2. A significant greenhouse gas output is gas, has sparked significant concern about its link to global warming and its potential contribution to issues like Acid rain, ur ban pollution, and health issues. In different contexts, such as space capsules, submarines, underground mining environments, or closed-circuit respiratory systems, removing CO2 produced within these closed ecological systems is crucial. Given these scenarios, CO2 removal has become a critical area of focus. Consequently, a range of methods for CO2 removal and separation from industrial waste gases, air, and gases resulting from animal metabolism, including human respiration, have been extensively researched and patented.

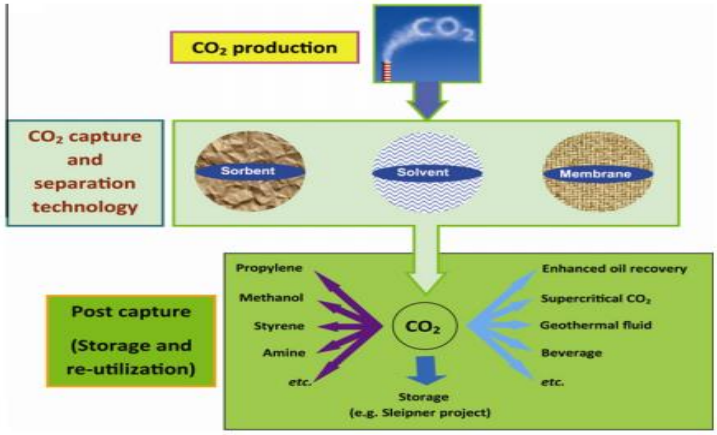

Figure 2 Schematic illustration showing the creation, capture, and storage or subsequent use of CO2

There are significant technical hurdles to overcome for the widespread adoption of power plants' CO2 capture. This involves simplified processes of CO2 generation, its capturing or splitting, and subsequent storage or reuse. CO2 is the most economically challenging step and encompasses two main technological approaches: pre-combustion, which involves capturing CO2 from the synthesis gas that has been reformed in a gasification unit prior to combustion, and post-burning, which comprises removing CO2 from the flue gas following combustion. CO2 can be captured and then stored underground to improve oil recovery or transformed into other valuable compounds as a carbon resource. Current CO2 capture and separation technologies primarily utilize solvents, sorbents, and membranes, with the capture mechanisms varying depending on the chemical properties of the capturing materials.

II. LITERATURE REVIEW

Zhou, K., et. al. (2020) [7] The Brayton cycle for supercritical carbon dioxide (S-CO2) has recently gained attention as an efficient and compact power cycle, potentially enhancing the economics of power plants. The turbine, a crucial component of this cycle, has not been extensively studied. This paper presents a design analysis with a focus on system optimization for a radial inflow turbine powered by S-CO2. For both design and off-design settings, computational fluid dynamics (CFD) simulations are run, together with a tip clearance study to evaluate turbine performance. Data from The NIST database is utilized to calculate the CO2 characteristics in the CFD analysis. The results show that the turbine has a total-to-static efficiency of 85.36% and a power output of 1.16 MW. Under nominal conditions, a minimal divergence of 3.73% between simulation and design results indicates the design model's trustworthiness. The turbine performs well in both design and off-design scenarios, according to numerical simulations. Additionally, the tip clearance analysis reveals that increasing the tip clearance by 6% leads to a decrease in turbine efficiency by 3.84% and a reduction in power output by 4.16%.

Kim, D. M., et. al. (2021) [8] In the pursuit of environmentally sustainable manufacturing, adopting eco-friendly cooling methods like cryogenic coolants is essential for machining operations, as opposed to traditional cutting fluids. The cryogenic spray technique, notably effective in lowering cutting temperatures and enhancing tool life during machining, stands out for its efficiency. Yet, there's limited research on its environmental and cost benefits in Hard turning processes with cryogenic assistance. This study investigates the environmental and economic impacts of employing liquid nitrogen as the coolant in cryogenic cooling for hard-turning operations. The study includes a computational fluid dynamics analysis and experimental validation to assess the efficiency of the spray method. It was determined that a nozzle with an internal angle of 45° is optimal for cryogenic spraying, delivering the furthest reach and a precise spray width, as confirmed by both computational analysis and experimental observations. The study also monitored When machining AISI 52100 steel (62 HRC), measure the flank wear lengths in wet, dry, and cryogenic settings. Ceramic cutting tool life was significantly increased by 3-6 times using the cryogenic procedure as opposed to dry and wet methods conditions. Additionally, the

economic impact was assessed using the extended tool-life data, revealing that the prolonged life of ceramic cutting tools under cryogenic conditions not only reduces total machine operation time but also cuts down on electricity usage and carbon dioxide emissions from machine operations. These findings suggest that cryogenic cooling is a viable option for green manufacturing, offering significant improvements in environmental impact.

Tsamos, K. M., et. al. (2017) [9] evaluates the effectiveness of four distinct CO2 refrigeration system configurations in retail food stores, focusing on their cooling efficiency, environmental footprint, energy usage, and yearly operational costs. The configurations assessed include the standard the complete gas bypass and CO2 cascade system, the booster refrigeration system with gas bypass (which serves as the standard), the booster system outfitted both the both a gas bypass compressor and an integrated cascade all-CO2 system without. The energy consumption and environmental impacts were modeled using the climatic conditions of London, UK (representing moderate climate) and Athens, Greece (representing a warmer climate). Control strategies for these systems were developed based on experimental laboratory tests conducted Regarding a conventional booster refrigeration setup. The findings revealed that the gas bypass compressor-equipped CO2 booster system delivers the most efficient performance, achieving energy savings of 5.0% in warmer climates and 3.65% in moderate climates. This was closely followed by the integrated cascade all CO2 system with a gas bypass compressor, which offered energy savings of For warm climates, the increase is 3.6% and 2.1% over the reference system, respectively.

Liu, B., et. al. (2022) [10] The supercritical carbon dioxide (SCO2) Brayton cycle sticks out as an incredibly promising method for improving waste heat from deliver exhaust gases. In this cycle, a published circuit heat exchanger (PCHE) is utilized due to its excessive performance and compact size. A observe turned into carried out to have a look at the observe centered at the thermal and hydraulic behavior of a Printed Circuit Heat Exchanger (PCHE) used as a precooler in a marine Supercritical CO2 (SCO2) Brayton cycle power technology device. To obtain this, a specialised PCHE checking out setup was created, which produced considerable data. This facts discovered that traditional heat transfer correlations do not appropriately seize the heat transfer dynamics of SCO2. As a end result, a simulation version based totally on computational fluid dynamics (CFD) became developed and proven with experimental statistics. Simulations were performed to evaluate the axial, radial, and normal thermal and hydraulic performance of the PCHE below the layout situations of the precooler in the marine Brayton cycle gadget. The CFD effects culminated in a brand new warmth switch correlation for SCO2, supplying essential theoretical insights for the layout of precoolers in sensible marine Brayton cycle power structur

Zheng, L., et. al. (2016) [11] introduces a dynamic model for a two-stage evaporation A refrigeration cycle utilizing a trans critical CO2 ejector expansion (EERC-TE), aimed at enhancing refrigeration cycle (EERC) operates. The model examines the impact of various disturbances, including adjustments in compressor hurry, development valve aperture, ejector nozzle throat area, and the flow rate of chilled water in the evaporators, on the system's transient responses. The results demonstrate a strong correlation with experimental data. Among the disturbances, changes in compressor speed have the most significant impact on system parameters. Alterations in the expansion valve opening notably affect the evaporator pressure and the ejector's pressure lift ratio, whereas modifications to the nozzle throat area of the ejector have a significant impact on the ejector entrainment ratio and the pressure of the gas cooler. These answers are similar in trend to those observed in the EERC system. From these transient results, combined adjustment strategies are suggested to enhance system performance. Notably, the improvement in the Coefficient of Show (COP) of EERC-TE is markedly more pronounced, being 2.58 eras higher than that of the EERC above the study's environments. The findings from these transient simulations provide a foundation for implementing versatile and effective adjustment methods to optimize system performance and inform system control strategies.

Lucas, C., et.al. (2014) [12] Incorporating an ejector into a vapor compression refrigeration system is a promising approach, with the system's performance significantly depending on the ejector's effectiveness. To enhance the understanding and design of two-phase CO2 ejectors, Computational Fluid Dynamics (CFD) simulations are extremely useful. This study employs a numerical model based on a homogeneous equilibrium approach, integrated within Open FOAM, to simulate the CO2 ejector. It includes a numerical analysis of the ejector's performance with and without a suction mass flow. The results are then compared with experimental data from prior studies for validation. Notably, when the ejector operates without a suction flow, it prevents mixing losses, making it an ideal scenario to verify the accuracy of the model in predicting friction losses, which are significant in this context. Subsequently, the model simulates an ejector with a suction flow to validate its ability to accurately predict mixing losses. Within the scope of the presented data, the model forecasts the driving mass flux with an error margin of about 10%. For an ejector operating without suction flow, the pressure recovery is estimated with a 10% error margin, which increases to 20% when operating with a suction flow. These findings highlight the model's capability and areas for potential refinement in predicting different operational aspects of CO2 ejectors.

III. OBJECTIVE

The main objective of the present work to enhance the heat transfer performance from the CO_2 fin tube gas cooler by mathematical and computational fluid dynamics analysis for various geometry and variable pitch of the CO_2 finned tube. There are following objective are as follows

- To perform the mathematical analysis to investigate the heat transfer coefficient and total heat transfer rate of the CO_2 finned tube.

- To perform the computational fluid dynamics analysis to predict the CO_2 refrigerant temperature profile along the tube from refrigerant inlet to outlet at different types of inlet velocity.
- To compare the results obtained from mathematical and computational fluid dynamics analysis and suggests better design of CO_2 finned tube gas cooler for better heat transfer.

IV. METHODLOGY

1.1 Mathematical Analysis

Velocity of the flowing fluid

$v = \frac{\dot{m}}{\rho . A_f}\ m/sec$

or

$\dot{m} = \rho . v . A_f$ Kg/Sec

Where

v = velocity in m/sec

$\dot{m}$ = Mass flow rate in kg/sec

ρ = Density in kg/m^3

A_f = Surface area of fin m^2

Surface Area of airside for different design of Co2 gas cooler:

Parameter	Value
Surface Area for Design-1	0.0208 m^2
Surface Area for Design-2	0.0209 m^2
Surface Area for Design-3	0.0209 m^2
Surface Area for Design-4	0.0211 m^2

Reynolds number

$R_e = \frac{\rho v D_o}{\mu}$

Nusselt number

$Nu = \frac{h.D_h}{k} = 0.023 Re^{0.8} Pr^{0.4}$

Where

h = Heat transfer coefficient (W/(m^2·K))

D_h = Hydraulic diameter (7.5 mm)

k = Thermal conductivity of the material

Coefficient of Heat Transfer

$h = \frac{Q_a}{A_f (T_i - T_{air})}$

Where

Q_a = Heat transfer rate (kW)

A_f = Area of fin m^2

T_i = Inlet Temperature [K]

T_{air} = Air Temperature [K]

The Colburn j-factor

$$j = \frac{Nu}{Re.Pr^{1/3}}$$

Where

Nu = Nusselt number

Re = Reynolds number

Pr = Prandelt number

Fanning f-friction factor

Characterized as the ratio of shear stress to flow kinetic energy density, the fanning friction factor (f) offers a correlation with the air pressure drop in passageways.

$$f = \frac{\Delta P.f_p}{2\rho v^2.L}$$

f_p = Fin Pitch [m] 1.5 mm

ΔP = Pressure Drop [Pa]

ρ = Density of the fluid [kg/m^3]

v = Fluid Velocity [m/sec]

L = Length of pipe (per meter length)

Filonenko correlation

$$f = (0.79ln.Re - 1.64)^{-2}$$

Gnielinski correlation: The CO2 heat transfer coefficient is computed using the Gnielinski correlation.

$$N_u = \frac{\left(f/8\right)(R_e - 1000)P_r}{\left(12.7\left(f/8\right)^{0.5} Pr^{0.66} - 1\right) + 1.07}$$

f = Friction Coefficient

d = Inner Diameter of Tube

L = Length of tube (per meter length)

When predicting the friction coefficient using filonenko's correlation,

The rate of heat transfer for refrigerant

$$Q_r = \dot{m}c_p(T_r^{in} - T_r^{out})$$

$$Q_r = h_r A(T_r^{in} - T_r^{out})$$

Q_r = Heat transfer from refrigerant

$\dot{m}$ = mass flow rate of refrigerant

c_p= Specific heat of refrigerant

h_r = Heat transfer coefficient of refrigerant

A = Area of refrigerant tube

T_r^{in} = Inlet temperature of refrigerant

T_r^{out} = Outlet temperature of refrigerant

Coefficient of performance of a refrigerator:

$$COP_{max} = \frac{T_{out}}{T_{in} - T_{out}}$$

Where

COP_{max} = coefficient of performance of refrigerator

T_{out} = Outlet Temperature of Refrigerant in degree Kelvin

T_{in} = Inlet Temperature of Refrigerant in degree Kelvin

Interpolation relation: the intermediates are found using the linear interpolation relation. values.

$$y = y_1 + (x - x_1)\frac{y_2 - y_1}{x_2 - x_1}$$

Table 2 Technical Parameter of CO_2 finned tube gas cooler *[X. Zhang et al. 2020]*

Dimensions	Value
W × H × D (m)	0.61 × 0.46 × 0.05
Front Area (0.61 × 0.46) (m^2)	0.2806
Fin Pitch (mm)	1.5
Fin Thickness (mm)	0.13
No. of Tubes row	03
Tube Diameter outside (mm)	7.9
Tube Diameter inside (mm)	7.5

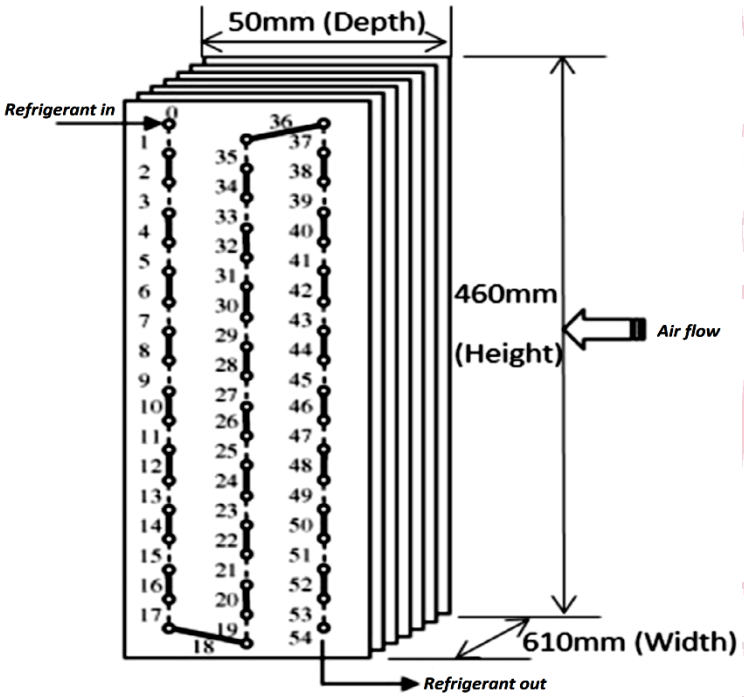

Figure 3 Geometry and dimension details of CO_2 finned tube gas cooler *[X. Zhang et al. 2020]*

1.2 CFD Analysis

CFD stands as a specialized domain within fluid mechanics, employing numerical analysis and data structures for the systematic examination and resolution of fluid flow-related predicaments. In the specific context the finned tube gas chiller for CO2 computational fluid dynamics analysis is conducted utilizing the ANSYS Fluent software. Input parameters, sourced from the foundational paper, guide this analytical process. The computational analysis necessitates the implementation of governing equations, encompassing the continuity equation, momentum equation, energy equations, as well as the K and ε equations.

A. Steps of computational fluid dynamics Analysis:

The distinct stages of analysis encompassed in (CFD) analysis are outlined below.

Preprocessor

- Creation of CAD Model:
- Generation of Meshing:
- Define Materials:

Solution Processor: At this stage of the study, the computer controls command and uses the finite element approach to solve the instantaneous equation.

Postprocessor: The general postprocessor is used to review analytic results for the entire model.

1.3 Algorithm used for Computational fluid dynamics analysis

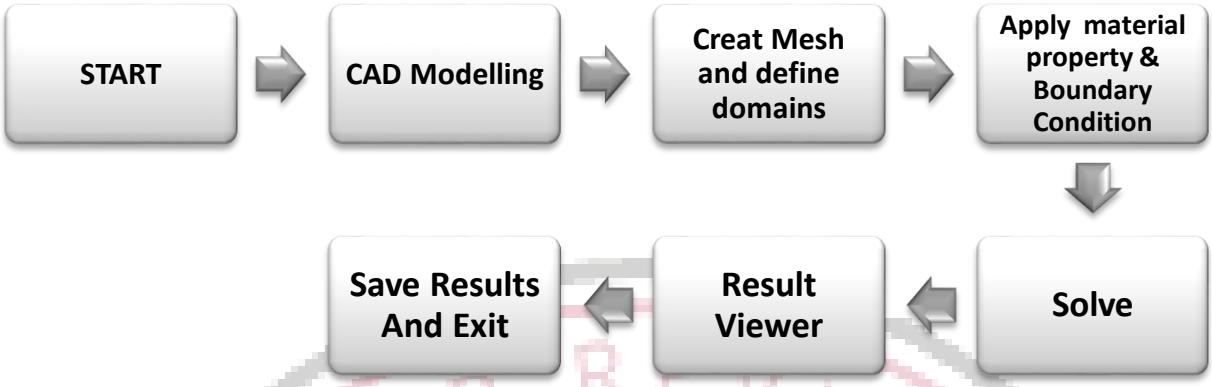

Figure 4 Algorithm used for Computational fluid dynamics analysis

1.4 Material Properties

Liquid carbon dioxide is a form of liquid resulting from the compression and cooling of gaseous carbon dioxide under high pressure. It does not naturally occur under standard atmospheric conditions; its existence is contingent on a pressure exceeding 5.2 bar and a temperature below 31.1 °C (critical point temperature) but higher than (-56.6 °C) (triple point temperature). Liquid carbon dioxide finds various applications, including the decaffeination of coffee, the extraction of virgin olive oil from olive paste, utilization in fire extinguishers, and as a coolant. Transparent and odorless, it possesses a density of 1101 kg/m3 when fully saturated at -37 °C.

Properties of liquid carbon dioxide (CO_2) *[engineeringtoolbox.com/CO2-carbon-dioxide-properties-d_2017.html]*

Table 3 At 90 bar density of liquid carbon dioxide (CO_2) *[Messer Group gases for life]*

Temperature *- T - (^oC)*	**Density** *- ρ - (kg/m^3)*	**Specific Heat** *- c_p - (KJ/kg K)*	**Thermal Conductivity** *- k - (W/m K)*	**Kinematic Viscosity** *- v - (10^{-6} m^2/s)*	**Prandtl's no.** *- Pr -*
-50	1156	1.84	0.086	0.119	2.96
-40	1118	1.88	0.101	0.118	2.46
-30	1077	1.97	0.112	0.117	2.22
-20	1032	2.05	0.115	0.115	2.12
-10	983	2.18	0.110	0.113	2.20
0	927	2.47	0.105	0.108	2.38
10	860	3.14	0.097	0.101	2.80
20	773	5.0	0.087	0.091	4.10
30	598	36.4	0.070	0.080	28.7

Properties of Air *[theengineeringmindset.com/properties-of-air-at-atmospheric-pressure]*

Temperature (T) ◦c	**Density (ρ) kg/m3**	**Dynamic Viscosity (μ) 10-5 kg/m.s**	**Specific Heat (cp) KJ/kg.K**	**Thermal Conductivity (k) W/m.K**	**Prandtl Number (Pr)**
-20	1.3958	1.6222	1.0054	0.022507	0.72467

-15	1.3687	1.6478	1.0054	0.022903	0.72337
-10	1.3426	1.6731	1.0055	0.023296	0.72212
-5	1.3175	1.6982	1.0055	0.023686	0.72092
0	1.2933	1.7231	1.0056	0.024073	0.71977
5	1.2699	1.7478	1.0057	0.024458	0.71866
10	1.2474	1.7722	1.0058	0.024840	0.71759
15	1.2257	1.7965	1.0059	0.025219	0.71657
20	1.2047	1.8205	1.0061	0.025596	0.71559
25	1.1845	1.8444	1.0063	0.025969	0.71465
30	1.1649	1.8680	1.0065	0.026341	0.71375
35	1.1459	1.8915	1.0067	0.026710	0.71289
40	1.1275	1.9148	1.0069	0.027076	0.71207
45	1.1098	1.9379	1.0072	0.027440	0.71128
50	1.0925	1.9608	1.0074	0.027801	0.71053
55	1.0759	1.9835	1.0077	0.028160	0.70982
60	1.0597	2.0061	1.0081	0.028517	0.70914
65	1.0439	2.0285	1.0084	0.028871	0.70849
70	1.0287	2.0507	1.0087	0.029223	0.70787
75	1.0139	2.0728	1.0091	0.029573	0.70729
80	0.99948	2.0947	1.0095	0.029921	0.70674
85	0.98549	2.1164	1.0099	0.030266	0.70622
90	0.97188	2.1380	1.0104	0.030609	0.70573
95	0.95865	2.1595	1.0108	0.030950	0.70527
100	0.94577	2.1808	1.0113	0.031289	0.70484

The CFD analysis relies on the following assumptions:

- The analysis is conducted under steady-state conditions.
- Curved surfaces are omitted to prevent meshing errors, leading to the simplification of tube fins as plain fins.
- Heat transfer coefficients remain consistent across each tube under constant air flow.
- The maximum temperature of the hot fluid is considered to be 360 K, a parameter not specified in the base paper.

1.5 Boundary Conditions

- To ascertain the temperature distribution, the energy equation is employed.
- Opt for the laminar flow viscous model.

- Utilize air as the working fluid for the airside fin, characterized by a density of 1.225 kg/m³. The fin material is aluminum with a thermal conductivity of k = 202.4 W/mK. Assume a uniform velocity profile for the airflow.
- The hot inlet of CO2 features a mass flow rate of 0.038 kg/sec and a temperature of 360 K.
- Consider air inlet velocities of 1, 2, and 3 m/sec, with an air inlet temperature of 302.55 K.
- Set the gauge pressure for the outlet boundary condition to zero.
- Treat all other surfaces as walls, imposing no-slip conditions for solid walls. For the outer side wall, set the heat flux as zero to establish an adiabatic condition.
- Apply the second-order upwind scheme for momentum, energy, turbulence, and dissipation rate.
- Employ the Fluent solver for conducting the CFD analysis.

1.6 Validation

The primary aim of this study is to improve the heat transfer efficiency of the CO2 finned tube gas cooler through mathematical and computational fluid dynamics analyses across different geometries of the gas cooler with finned tubes for CO2. For the validation of the present work an research paper of *Xinyu Zhang et al. (2020) "Analysis of the finned-tube CO2 gas coolers' CFD performance with different inlet air flow patterns" https://doi.org/10.1016/j.enbenv.2020.02.004 Energy and Built Environment 1 (2020) 233–241* has been studies and performed computational fluid dynamics analysis by using CAD model of the length and width of the finned tube gas cooler is 610 mm × 50 mm with 0.13 mm fin thickness, the outer and inner diameter of tube is 7.9 mm & 7.5 mm with 1.5 mm with 03 rows of tubes. Following the completion of computational fluid dynamics analysis, the obtained results have been compared and validated against existing literature.

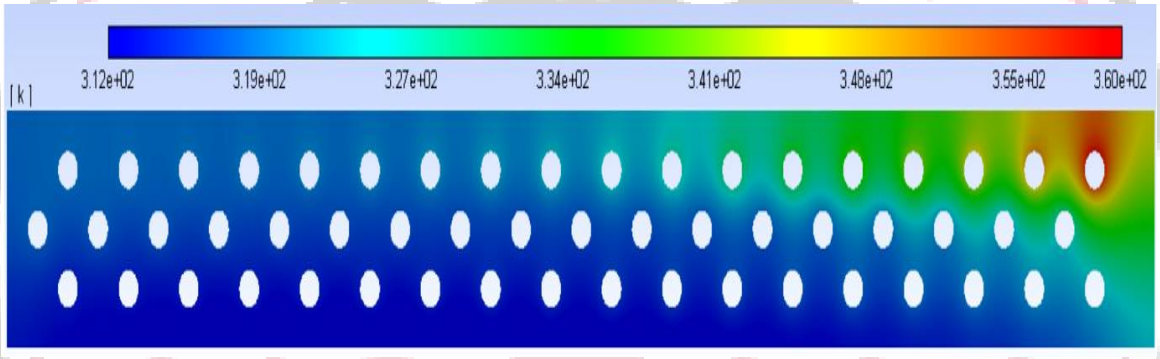

Figure 5 Temperature distribution of the middle fin surface for the parabolic airflow velocity profiles at 1 m/sec *[X. Zhang et al 2020]*

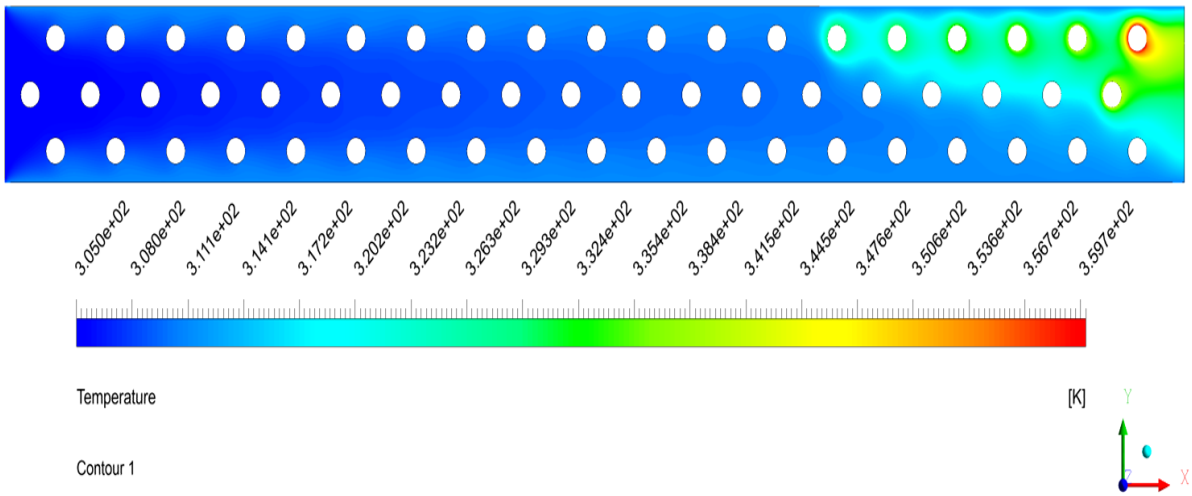

Figure 6 Temperature distribution of the middle fin surface for the parabolic airflow velocity profiles at 1 m/sec *[Present work]*

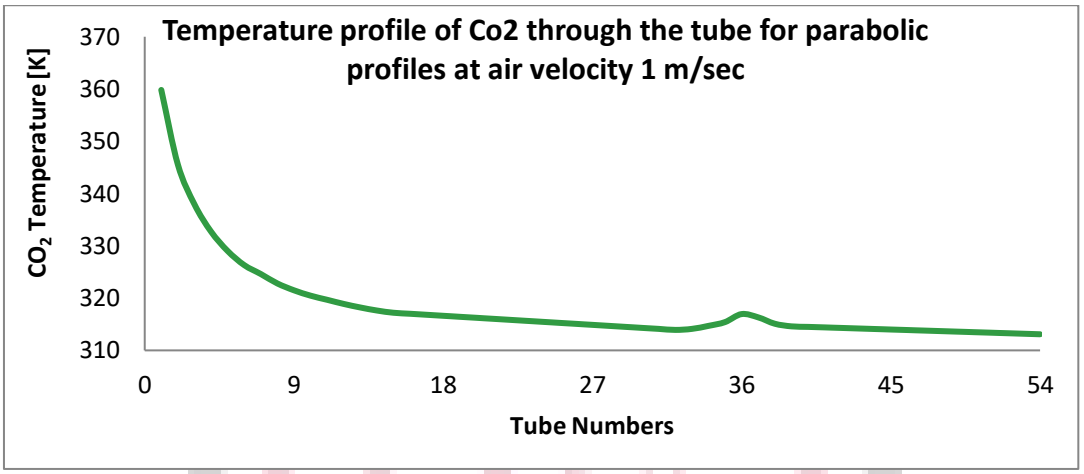

Figure 7 Temperature profile of Co_2 through the tube for parabolic profiles at air velocity 01 m/sec *[Present work]*

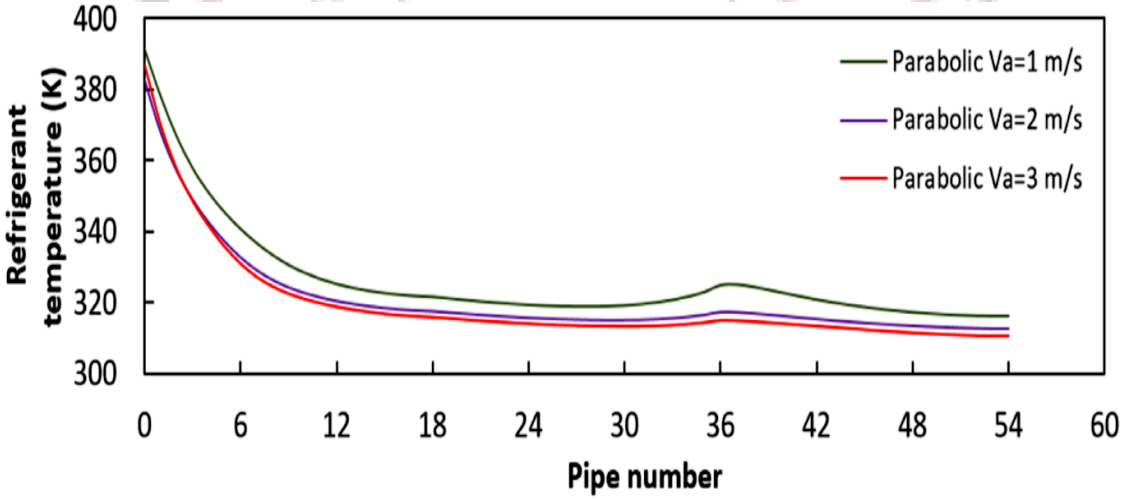

Figure 8 Temperature profile of Co_2 through the tube for parabolic profiles at air velocity 1,2 & 3 m/sec *[X. Zhang et al 2020]*

From the above contours and graphical diagram it has been observed that maximum temperature variation in present work is 0.08% and minimum temperature variation is 0.335% as compared with base paper. All above compared results show very good agreement between base paper and present work, hence the further analysis for different design of Co_2 gas cooler with same boundary conditions have to be done.

V. RESULT AND DISCUSSION

In the present study, computational fluid dynamics analysis as well as mathematical analysis were conducted to assess various designs of CO2 finned tube gas coolers with the aim of enhancing thermal performance. The primary objective is to improve the heat transfer efficiency of the CO2 fin tube gas cooler through mathematical and computational fluid dynamics analyses across different geometries of the CO2 finned tube gas cooler. Four CFD models were developed for this purpose, facilitating the evaluation and comparison of heat exchanger performance under different inlet airflow uniform velocity profiles. The subsequent chapter delves into a comprehensive discussion of the results derived from the mathematical and computational fluid dynamics analyses for all the designs considered.

5.1 Mathematical Result Analysis

Velocity of the flowing fluid:

$v = \frac{\dot{m}}{\rho . A_f}\ m/sec$

$\dot{m} = \rho . v . A_f$ Kg/Sec

Mass flow rate of air at 1 m/sec for different design [Kg/Sec]	Mass flow rate of air at 2 m/sec for different design [Kg/Sec]	Mass flow rate of air at 3 m/sec for different design [Kg/Sec]
0.02548	0.05096	0.07644
0.025603	0.051205	0.076808
0.025603	0.051205	0.076808
0.025848	0.051695	0.077543

Nusselt number

$Nu = \frac{h.D_h}{k} = 0.023Re^{0.8}Pr^{0.4}$

h = Heat transfer coefficient (W/(m^2·K))

D_h = Hydraulic diameter

Hydraulic diameter can be calculated as

$D_h = \frac{2ab}{a+b}$

a = length of fin (0.46 m)

b = width of the fin (0.05 m)

$D_h = \frac{2\times0.46\times0.05}{0.46+0.05} = 0.0902\,m$

k = Thermal conductivity of the material

$Nu = \frac{47.71\times0.0902}{0.0252} = 170.77$

$Nu = \frac{188.2\times0.0902}{0.0252} = 673.64$

$Nu = \frac{282.3\times0.0902}{0.0252} = 1010.45$

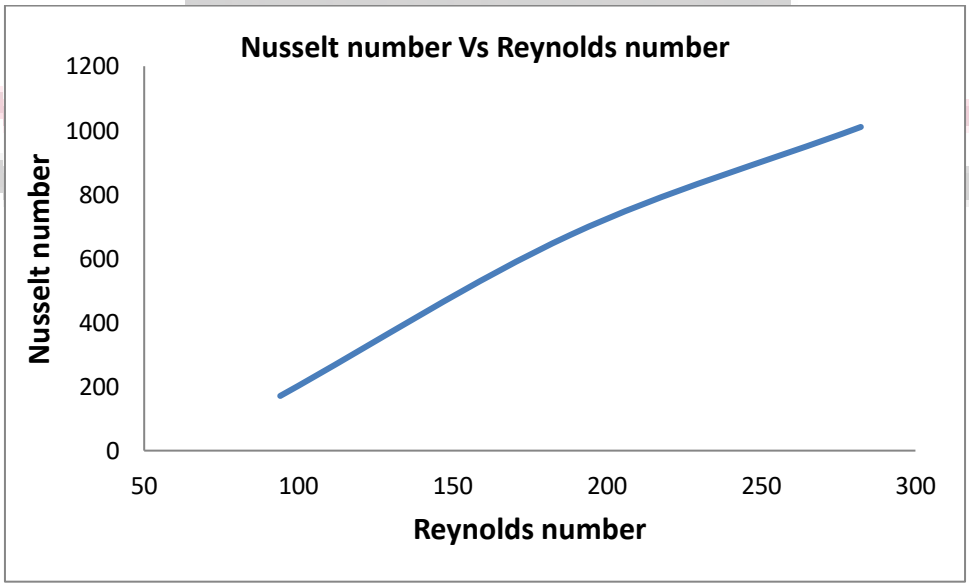

Figure 9 Nusselt number Vs Reynolds number

Heat transfer coefficient

$h = \frac{Q_a}{A_f(T_i - T_{air})}$

Where

Q_a = Heat transfer rate (kW)

A_f = Area of fin m^2

T_i = Inlet Temperature [K]

T_{air} = Air Temperature [K]

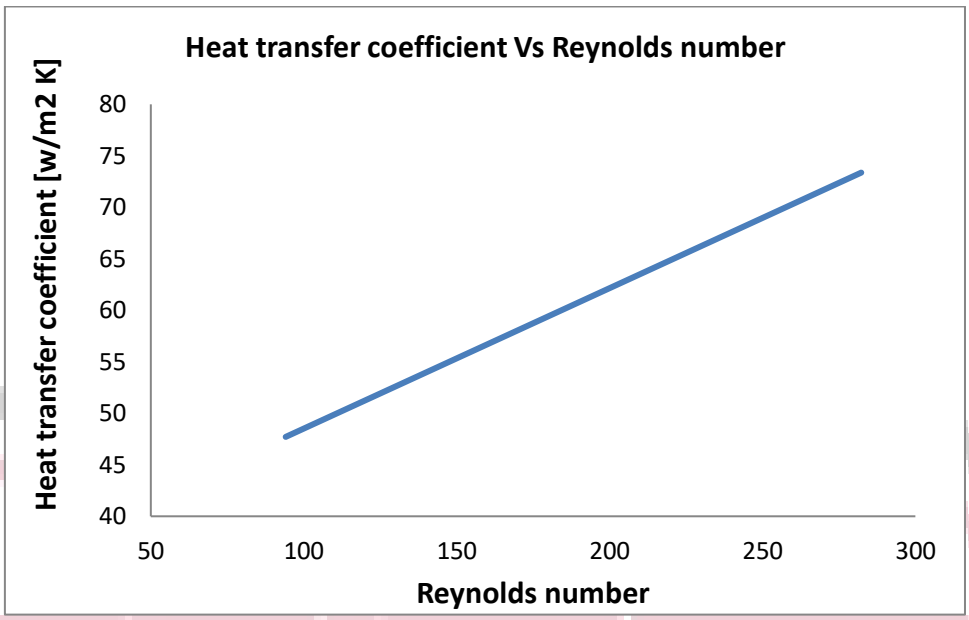

Figure 10 Heat transfer coefficient Vs Reynolds number

The Colburn j-factor

$j = \frac{Nu}{Re.Pr^{1/3}}$

Nu = Nusselt number

Re = Reynolds number

Pr = Prandelt number

Filonenko correlation

$f = (0.79ln.Re - 1.64)^{-2}$

$f = (0.79ln.94.1 - 1.64)^{-2} = \mathbf{0.26297}$

$f = (0.79ln.188.2 - 1.64)^{-2} = \mathbf{0.1603}$

$f = (0.79ln.282.3 - 1.64)^{-2} = \mathbf{0.12593}$

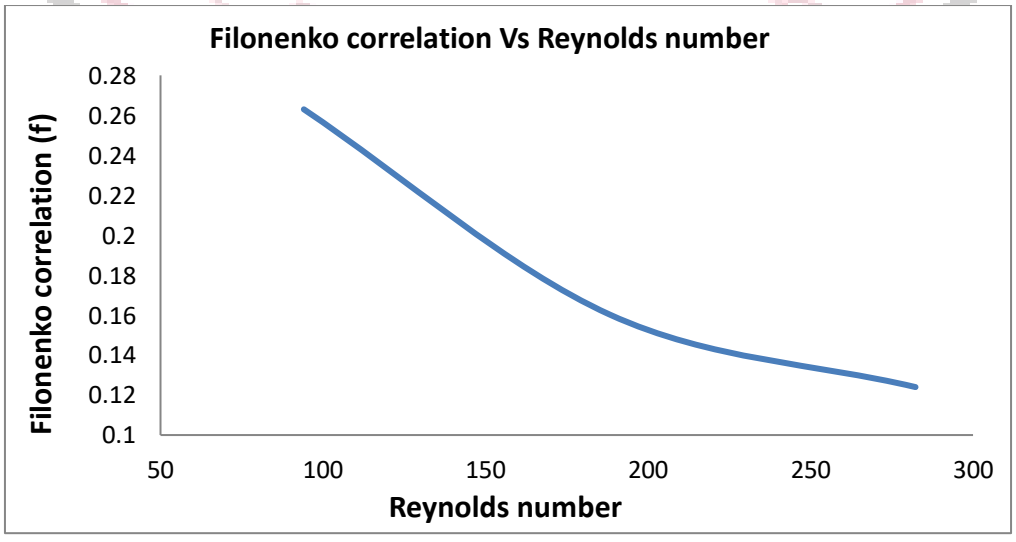

Figure 11 Filonenko correlation Vs Reynolds number

Fanning f-friction factor

The ratio of shear stress to the flow kinetic energy density is known as the fanning friction factor (f), and it correlates to the pressure drop that air experiences in passageways.

$f = \frac{\Delta P.f_p}{2\rho v^2.L}$

f_p = Fin Pitch [m] 0.0015

ΔP = Pressure Drop [Pa]

ρ = Density of the fluid [kg/m^3]

v = Fluid Velocity [m/sec]

L = Length of pipe (per meter length)

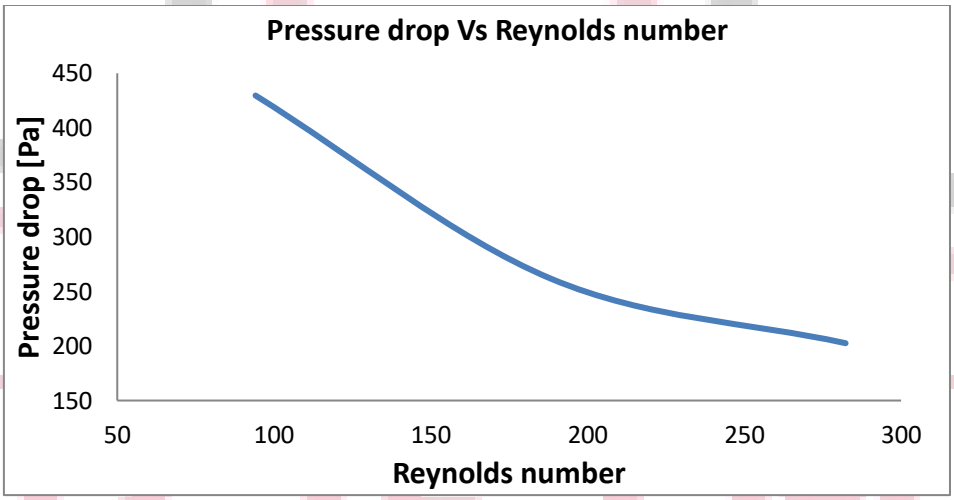

Figure 12 Pressure drop Vs Reynolds number at different flow rate

Gnielinski correlation: The Gnielinski correlation is employed to compute the heat transfer coefficient for CO2.

The Gnielinski Correlation is valid for

$0.5 \leq Pr \leq 2000$

$3000 \leq Re \leq 5 \times 10^6$

$N_u = \frac{\left(f/8\right)(R_e - 1000)P_r}{\left(12.7\left(f/8\right)^{0.5} Pr^{0.66} - 1\right) + 1.07}$

f = Friction Coefficient

d = Inner Diameter of Tube

L = Length of tube (per meter length)

$N_u = \frac{(0.263/8)\times(94.1-1000)\times 3.978}{\left(12.7\times(0.263/8)^{0.5}\times 3.978^{0.66}-1\right)+1.07} = -20.4324$

$N_u = \frac{(0.1603/8)\times(188.2-1000)\times 1.957}{\left(12.7\times(0.1603/8)^{0.5}\times 1.957^{0.66}-1\right)+1.07} = -11.0914$

$N_u = \frac{(0.124/8)\times(282.3-1000)\times 0.141}{\left(12.7\times(0.124/8)^{0.5}\times 0.141^{0.66}-1\right)+1.07} = -3.1124$

Where, Filonenko's correlation is used to predict the friction coefficient,

The heat transfer rate for refrigerant

$Q_r = h_r A(T_r^{in} - T_r^{out})$

Q_r = Heat transfer from refrigerant

$\dot{m}$ = mass flow rate of refrigerant

c_p= Specific heat of refrigerant

h_r = Heat transfer coefficient of refrigerant

A = Area of refrigerant tube

T_r^{in} = Inlet temperature of refrigerant

T_r^{out} = Outlet temperature of refrigerant

$Q_r = \dot{m}c_p(T_r^{in} - T_r^{out})$

Refrigerant heat transfer rates for different designs are computed as follows:

For design-1:

$Q_{r,Design-1} = 0.038 \times 840.37(360 - 305) = 1756.373\ Watt$

For design-2:

$Q_{r,Design-2} = 0.038 \times 840.37(360 - 305) = 1820.241\ Watt$

For design-3:

$Q_{r,Design-3} = 0.038 \times 840.37(360 - 305) = 1947.978\ Watt$

For design-4:

$Q_{r,Design-4} = 0.038 \times 840.37(360 - 305) = 2107.648\ Watt$

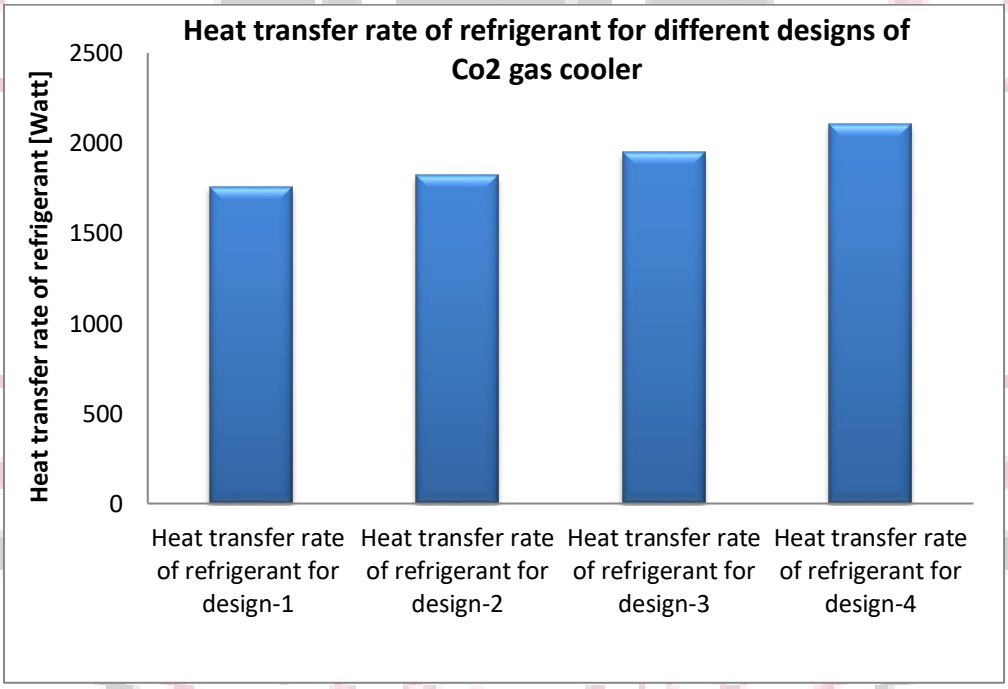

Figure 13 Heat transfer rate of refrigerant for different designs of Co_2 gas cooler

Table 4 Heat transfer rate from airside for different designs of Co_2 Gas Cooler

Reynolds number	Heat transfer rate from airside for design-1	Heat transfer rate from airside for design-2	Heat transfer rate from airside for design-3	Heat transfer rate from airside for design-4
94.1	55.58024	57.83692	61.82548	67.44095
188.2	70.25776	73.1213	78.18245	85.308
282.3	84.93528	88.40568	94.53941	103.1751

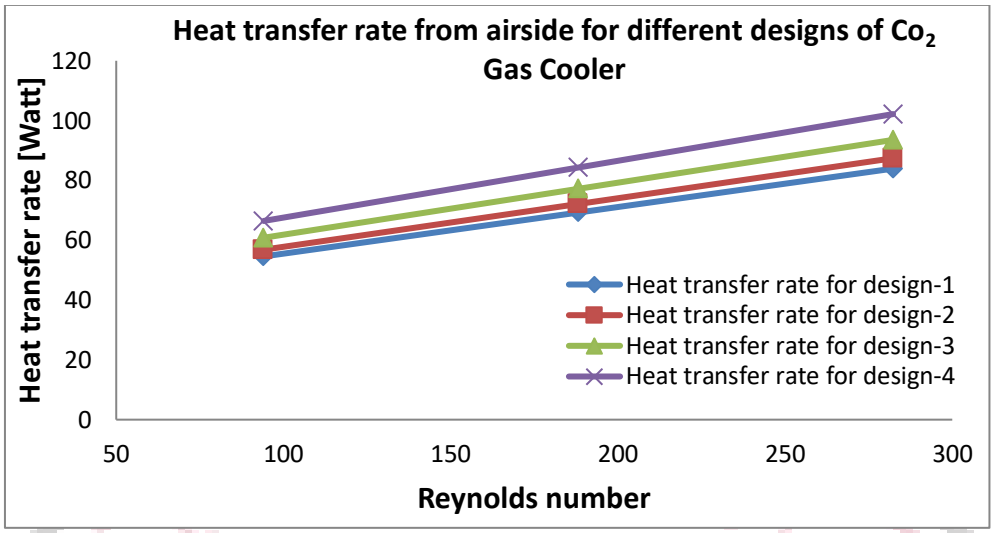

Figure 14 Heat transfer rate from airside for different designs of Co_2 Gas Cooler

Based on the mathematical analysis above, it is evident that the airside heat transfer coefficient rises When the Reynolds number rises from 94.1 to 282.3 with a uniform airflow profile, the value of 47.71 W/m² K to 73.37 W/m² K is observed.

Table 5 Comparison of Temperature Distribution across the Entire Fin Surface for Various Designs

Velocity	Design-1		Design-2		Design-3		Design-4	
	Max. Temperature	Min. Temperature	Max. Temperature	Min. Temperature	Max. Temperature	Min. Temperature	Max. Temperature	Min. Temperature
At 1 m/sec	359.7	305	359.5	303	359.7	299	359.8	294
At 2 m/sec	359.7	306.8	359.5	304.6	359.7	302.3	359.8	298.3
At 3 m/sec	359.7	308.1	359.5	306.4	359.7	304.7	359.8	300

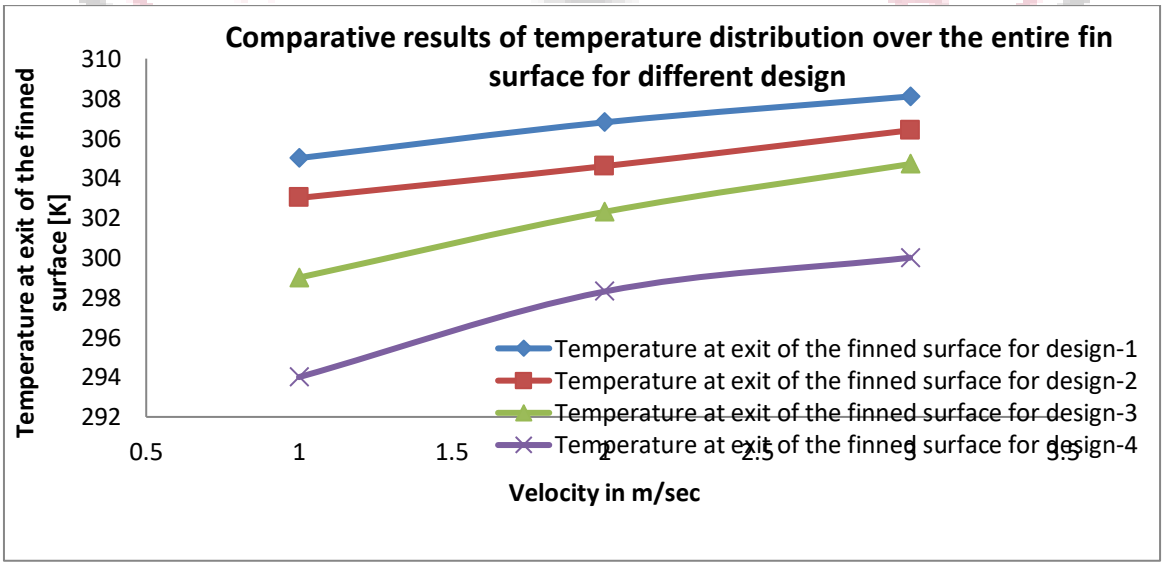

Figure 15 Comparative results of temperature distribution over the entire fin surface for different design

Analyzing the comparative results of temperature distribution across the entire fin surface for various designs, it is noted that as the airflow increased from 1 m/s to 3 m/s, the temperature difference decreased, leading to a reduction in heat transfer. The graph above indicates that design-4 of the CO2 finned tube gas cooler exhibits the highest temperature drop, implying a more efficient heat transfer rate. It is also observed that design-4 achieved a maximum temperature drop of 65.8 K.

Table 6 Comparative results of Heat transfer rate of refrigerant for different design

Velocity	Heat transfer rate of refrigerant for design-1 [watt]	Heat transfer rate of refrigerant for design-2 [watt]	Heat transfer rate of refrigerant for design-3 [watt]	Heat transfer rate of refrigerant for design-4 [watt]
At 1 m/sec	1646.793	1704.274	1838.397	2001.261
At 2 m/sec	1589.312	1653.18	1733.015	1863.945
At 3 m/sec	1547.797	1595.699	1656.373	1809.657

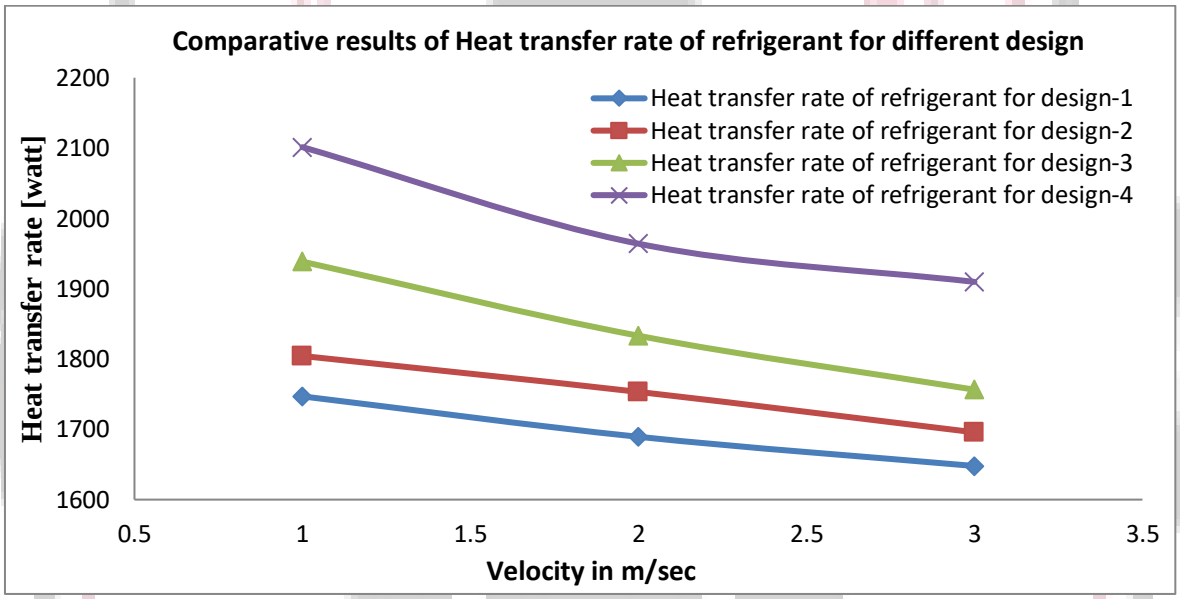

Figure 16 Comparing Heat Transfer Rates of Refrigerant across Various Designs

Analyzing the comparative results of the heat transfer rate of the refrigerant for different designs reveals that an increase in airflow from 1 m/s to 3 m/s led to a reduction in the heat transfer rate. The accompanying graph indicates that design-4 of the CO2 finned tube gas cooler attained the highest heat transfer rate.

Table 7 Enhanced Performance of CO2 Finned Tube Gas Cooler Across Various Designs Compared to the Base Design

Velocity	Performance improvement of Design-2 as compared with base design	Performance improvement of Design-3 as compared with base design	Performance improvement of Design-4 as compared with base design
At 1 m/Sec	3.29	9.97	19.29
At 2 m/Sec	2.78	7.51	15.26
At 3 m/Sec	1.91	5.59	14.89

Upon examining the comparative results concerning the performance improvement of the CO2 finned tube gas cooler across various designs in contrast to the base design, it becomes apparent that design-4 provides the most significant performance enhancement. It demonstrates a 20.29% improvement compared to design-1. For design-3, there is a 10.97% improvement over the base design, and design-2 shows a 3.29% improvement over the base design.

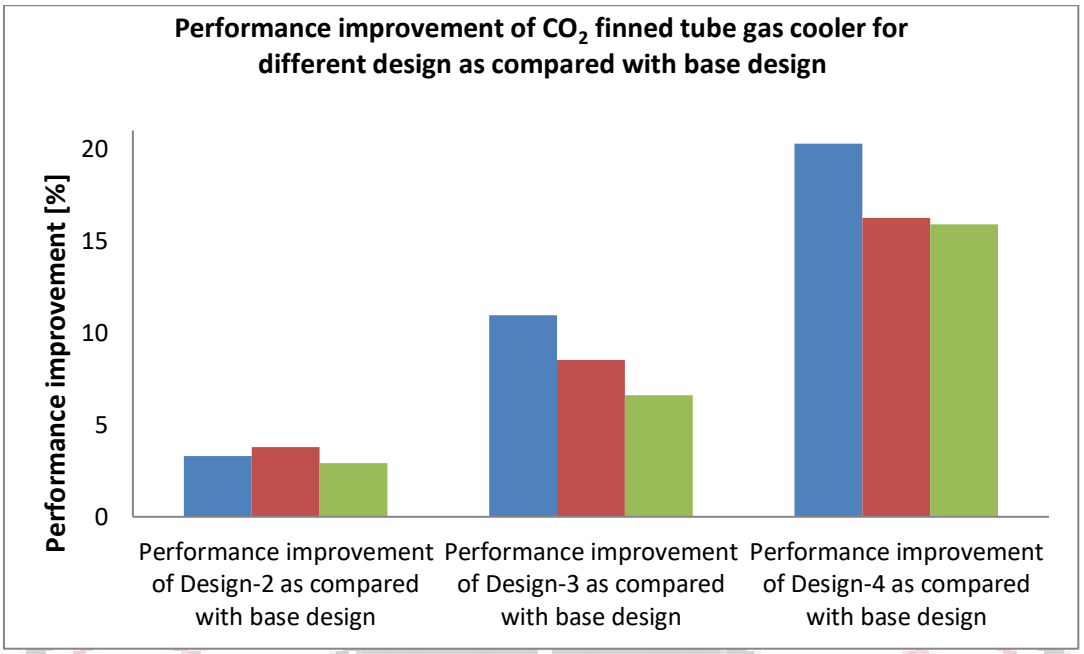

Figure 17 Enhancement in the performance of CO2 finned tube gas coolers across various designs in comparison to the base design.

VI. CONCLUSION

The study concludes with significant advancements in the design and performance of CO2 finned tube gas coolers. Through detailed mathematical and CFD analyses, the paper demonstrates improved heat transfer efficiency in various cooler designs, particularly in high-temperature environments. The research underscores the importance of optimized gas cooler layouts and operation, with a focus on geometrical parameters and airflow conditions. The findings highlight the effectiveness of different fin geometries in enhancing heat transfer rates and suggest design-4 of the CO2 finned tube gas cooler as the most efficient, achieving the highest temperature drop. This work contributes to the development of more sustainable and efficient cooling systems, addressing both environmental concerns and the need for high-performance cooling solutions in diverse climatic conditions.

REFERENCES

[1] Lata, M., & Gupta, D. K. (2021). Simulation and performance evaluation of trans-critical CO2 refrigeration system with modified evaporative cooled finned tube gas cooler in Indian context. *Applied Thermal Engineering*, *186*, 116500. https://doi.org/10.1016/j.applthermaleng.2020.116500

[2] Zhang, X., Ge, Y., & Sun, J. (2020). CFD performance analysis of finned-tube CO2 gas coolers with various inlet air flow patterns. *Energy and Built Environment*, *1*(3), 233-241.

[3] Santosa, I. D. (2015). *Optimisation gas coolers for CO2 refrigeration application* (Doctoral dissertation, Brunel University London).

[4] Tao, Y.B.; He, Y.L.; Tao, W.Q. Exergetic analysis of transcritical CO2 residential air-conditioning system based on experimental data. *Appl. Energy* **2010**, *87*, 3065–3072.

[5] Alexopoulos, C.; Aljolani, O.; Heberle, F.; Roumpedakis, T.C.; Brüggemann, D.; Karellas, S. Design Evaluation for a Finned-Tube CO_2 Gas Cooler in Residential Applications. *Energies* 2020, *13*, 2428. https://doi.org/10.3390/en13102428

[6] Li, B., Duan, Y., Luebke, D., & Morreale, B. (2013). Advances in CO2 capture techn 3ology: A patent review. *Applied Energy*, *102*, 1439-1447. https://doi.org/10.1016/j.apenergy.2012.09.009

[7] Zhou, K., Wang, J., Xia, J., Guo, Y., Zhao, P., & Dai, Y. (2020). Design and performance analysis of a supercritical CO2 radial inflow turbine. *Applied Thermal Engineering*, *167*, 114757.https://doi.org/10.1016/j.applthermaleng.2019.114757

[8] Kim, D. M., Kim, H. I., & Park, H. W. (2021). Tool wear, economic costs, and CO2 emissions analysis in cryogenic assisted hard-turning process of AISI 52100 steel. *Sustainable Materials and Technologies*, *30*, e00349. https://doi.org/10.1016/j.susmat.2021.e00349

[9] Tsamos, K. M., Ge, Y. T., Santosa, I., Tassou, S. A., Bianchi, G., & Mylona, Z. (2017). Energy analysis of alternative CO2 refrigeration system configurations for retail food applications in moderate and warm climates. *Energy Conversion and Management*, *150*, 822-829.https://doi.org/10.1016/j.enconman.2017.03.020

[10] Liu, B., Lu, M., Shui, B., Sun, Y., & Wei, W. (2022). Thermal-hydraulic performance analysis of printed circuit heat exchanger precooler in the Brayton cycle for supercritical CO2 waste heat recovery. *Applied Energy*, *305*, 117923.https://doi.org/10.1016/j.apenergy.2021.117923

[11] Zheng, L., Deng, J., & Zhang, Z. (2016). Dynamic simulation of an improved transcritical CO2 ejector expansion refrigeration cycle. *Energy Conversion and Management*, *114*, 278-289. https://doi.org/10.1016/j.enconman.2016.01.069

[12] Lucas, C., Rusche, H., Schroeder, A., & Koehler, J. (2014). Numerical investigation of a two-phase CO2 ejector. *International journal of refrigeration*, *43*, 154-166. https://doi.org/10.1016/j.ijrefrig.2014.03.003

[13] Belov, I., Vermeiren, V., Paulussen, S., & Bogaerts, A. (2018). Carbon dioxide dissociation in a microwave plasma reactor operating in a wide pressure range and different gas inlet configurations. *Journal of CO2 Utilization*, *24*, 386-397. https://doi.org/10.1016/j.jcou.2017.12.009